Epitaxial ZnO thin films grown by pulsed electron beam deposition

S. Tricot [a,*], M. Nistor [b], E. Millon [a], C. Boulmer-Leborgne [a], N.B. Mandache [b], J. Perrière [c], W. Seiler [d]

[a] GREMI, UMR 6606 CNRS/Université d'Orléans, 14 rue d'Issoudun, B.P. 6744, 45067 Orléans Cedex 2, France
[b] National Institute for Lasers, Plasma and Radiation Physics, PO Box MG-36, Bucharest-Magurele, Romania
[c] INSP, UMR 7588 CNRS/Université Pierre et Marie Curie - Paris 6, 140 rue de Lourmel, 75015 Paris, France
[d] PIMM, UMR 8006 CNRS/ENSAM, 151 Boulevard de l'Hôpital, 75013 Paris, France

Keywords:
Pulsed electron beam deposition (PED)
Zinc oxide
Pole figure
Resistivity
Tauc plot

A B S T R A C T

In this work, the pulsed electron beam deposition method (PED) is evaluated by studying the properties of ZnO thin films grown on *c*-cut sapphire substrates. The film composition, structure and surface morphology were investigated by means of Rutherford backscattering spectrometry, X-ray diffraction and atomic force microscopy. Optical absorption, resistivity and Hall effect measurements were performed in order to obtain the optical and electronic properties of the ZnO films. By a fine tuning of the deposition conditions, smooth, dense, stoichiometric and textured hexagonal ZnO films were epitaxially grown on (0001) sapphire at 700 °C with a 30° rotation of the ZnO basal plane with respect to the sapphire substrate. The average transmittance of the films reaches 90% in the visible range with an optical band gap of 3.28 eV. Electrical characterization reveals a high density of charge carrier of 3.4×10^{19} cm^{-3} along with a mobility of 11.53 cm²/Vs. The electrical and optical properties are discussed and compared to ZnO thin films prepared by the similar and most well-known pulsed laser deposition method.

1. Introduction

Pulsed electron beam deposition (PED) is a recent and simple method for deposition of thin films. In PED, a pulsed electron beam is used to ablate the surface of a target material and the emitted species are collected onto a substrate in front of the target [1,2]. The PED setup is thus very similar to the pulsed laser deposition technique (PLD).

In a previous paper we showed that whatever the nature, composition and properties of the materials grown by PED, particulates of the order of tens-hundred of nm in diameter are present at the surface of the thin films, but by a careful optimization of the electron beam parameters it is possible to drastically reduce the density and size of particulates at the surface of the films [2]. This could be explained by a unique feature of the pulsed-beam which delivers electrons with a large energy distribution, with a dominant high-energy electron component at earlier times and a contribution of lower energy electrons increasing towards later times [3–5].

The investigation of the plasma plume produced by the pulsed electron beam with the target by fast imaging and optical emission spectroscopy [3,5] showed that the kinetic energies of the species emitted by the target is about 10–50 eV, thus enhancing the adatom mobility when arriving on the substrate surface and providing enough energy to enhance the film growth while avoiding surface droplets.

One interesting aspect of the PED method is its ability to ablate a wide range of target materials and especially wide band gap semiconductors that are more difficult to process by PLD since they are poorly absorbent to the laser light. Zinc oxide (ZnO) is an example of such materials and it has already been shown that ZnO thin films grown by PLD are of better quality when prepared using a laser wavelength shorter than the band gap of ZnO [6]. Thus, PED could be an alternative to PLD for large band gap materials.

Moreover, ZnO has very attractive properties. It is a natural n-type semiconductor with resistivity values ranging from 10 to 10^{-2} Ω/cm [7] for undoped ZnO. Optical properties of ZnO also focus intense research due to its wide direct band gap of 3.3 eV which makes ZnO transparent to the visible light. Its properties makes therefore ZnO promising for applications in optoelectronics, piezoelectric devices, SAW filters, gas sensors, solar cell transparent electrodes, transparent electronics and spintronics [7–9]. Some of these applications require very well-crystallized ZnO thin films or even ZnO epitaxially grown on a substrate. However, the growth of ZnO films by PLD is now well optimized [10] but despite the large number of data already reported in the literature on the structural and physical properties of ZnO films grown under various experimental conditions, very few studies give an accurate description of ZnO films grown by PED [11].

In this work, we investigate the morphological, structural, optical and electrical properties of ZnO thin films prepared by PED. The aim is to compare these films with known results from the literature of PLD prepared ZnO films to know if PED could be a reliable alternative to PLD for wide band gap materials. To hold a comparison of both techniques and to be only sensitive to the deposition process, growths

* Corresponding author.
E-mail address: sylvain.tricot@univ-rennes1.fr (S. Tricot).

were performed on sapphire (000*l*) substrate held at 700 °C without any post-treatment. These conditions — classically reported in PLD — are known to give well crystallized and epitaxied films.

2. Experimental

ZnO thin films were grown by the PED method on *c*-cut sapphire (0001) single crystal substrates. The experimental set-up of PED, described in detail in previous papers [2,5] is sketched in Fig. 1. Basically, a pulsed-electron beam interacts with a solid ZnO target and induces a plasma. The ablated species are collected onto the substrate facing the target and a thin film is formed pulses after pulses much like the pulsed laser deposition technique. The produced electron beam pulse width is 100 ns (FWHM), the total current reaches 800 A and it is composed of electrons with energies ranging from a few eV to the energy corresponding to the applied high voltage (15 keV for an applied voltage of −15 kV for example). The beam diameter is in the 2–4 mm range leading to a fluence of about 2.5 J/cm². The electron beam source consists of a hollow cathode, a dielectric capillary tube (6 mm in diameter and 110 mm in length) and the vacuum chamber as grounded anode. At each pulse, a 16 nF external capacitor is discharged between the cathode and the anode. The discharge voltage was varied in the 14–16 kV range. The maximum pulse repetition rate of the device is 5Hz and was kept at 1Hz for these experiments. The target-substrate distance is set to 40 mm and the substrate was heated at 700 °C. Indeed growth temperatures higher than 300 °C is known to favor a better crystallinity of films [7]. During the film growth the argon pressure was kept at 1.4×10^{-2} mbar inside the chamber. This argon pressure is needed for the electron beam operation. After the growth, films are cooled down in the ablation chamber under the same argon pressure.

Rutherford backscattering spectrometry, using 2 MeV energy $^4He^+$ ion beams from the Van de Graaff accelerator of the Institut des NanoSciences de Paris (INSP-Université Paris 6) was used to measure the thickness and composition of the zinc oxide films. The accurate determination of the in-depth distribution of the elements in films was obtained by the RUMP simulation program [12]. Due to the low RBS yield on oxygen, the relative accuracy of this element in films was therefore close to 4%. The surface morphology of films was investigated by atomic force microscopy. The structural characterizations of the zinc oxide films were carried out by XRD analyses using a four circle diffractometer (Philips Xpert MRD of LIM laboratory-ENSAM-Paris) with the Cu Kα radiation (λ = 0.154 nm). The nature of the crystalline phases, their axis parameters and their preferred orientations with respect to the substrates were investigated by XRD experiments in the Bragg–Brentano geometry. The in-plane epitaxial relationships between films and single crystal substrates were studied by asymmetric diffraction with the measurements of pole figures of selected reflection peaks of the film and substrates. The optical absorption of films was measured in the 200–2500 nm range with a Cary 5000 spectrophotometer. To obtain a better understanding of the properties of excitons in ZnO thin films, photoluminescence measurements were carried out at room temperature using a xenon lamp as excitation source at λ = 350 nm. The transport properties (resistivity as a function of temperature from room temperature down to liquid He temperature) of the zinc oxide films were obtained by the classical four probe method. The carrier type and concentration as well as their mobility were determined with a MMR Hall measurement system in the Van der Pauw geometry at a magnetic field of 0.3 T.

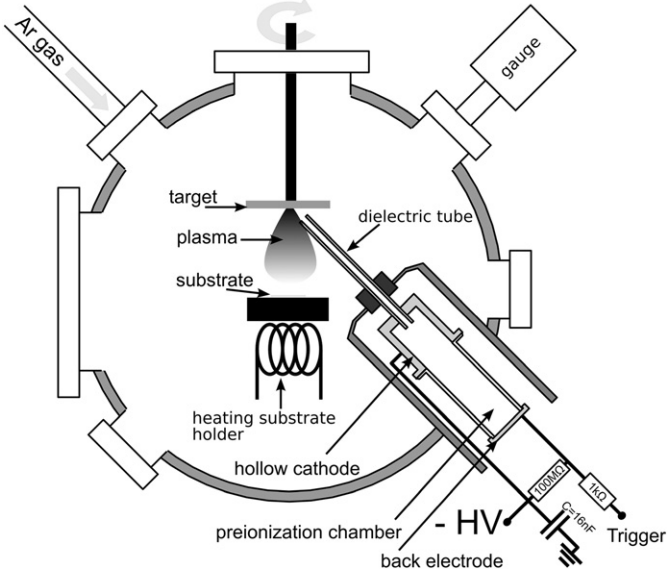

Fig. 1. Top view of the PED experimental setup. The dielectric tube defines an angle of 45° with the target.

3. Results and discussion

3.1. Film composition and morphology

Parameters of the pulsed-electron beam for the growth of zinc oxide films were optimized in order to obtain the formation of dense and smooth zinc oxide films free of particulates. The RBS spectra recorded on such zinc oxide films grown on *c*-cut sapphire substrate at 700 °C evidenced that no interdiffusion occurs between the film and the substrate and that the surface roughness is smooth. A uniform in-depth distribution of Zn and O species was also observed in the films, leading to the conclusion that nearly stoichiometric ZnO films are formed in these conditions. Moreover, argon incorporation in the zinc oxide films was not evidenced despite the fact these films were grown under a relatively high argon partial pressure (1.4×10^{-2} mbar). This point is one of the main specificity of the PED growth method with respect to other growth methods like conventional sputtering which lead to argon incorporation in the films during growth under similar argon pressure [13]. In PED, growth occurs in presence of an argon plasma whose species (Ar ions or atoms) have a low kinetic energy (maximum a few eV). Such species can be physically adsorbed at the surface or in the near surface region of the growing film. Meanwhile, species directly emitted by the target during and after the electron bombardment fly to the substrate with large kinetic energies (in the tens of eV range) [2,5]. In these conditions, the bombardment of the film surface with the energetic target species induces the desorption of any weakly adsorbed species like Ar which could be incorporated. Thus, the ZnO films grown by PED are free from argon. It is worth noticing that ZnO films prepared by PLD are usually grown under an oxygen partial pressure that can be varied in a wide range from 10^{-5} to 10^{-1} mbar. Without addition of oxygen during the growth, the resulting films are zinc enriched. Thanks to the optimization of the discharge parameters, we showed here that it is possible to obtain nearly stoichiometric ZnO thin film by PED without adding oxygen in the chamber.

It is also important to note that the growth rate of the PED technique is in the 0.05–0.11 nm/pulse range which is more than 10 times greater than those classically obtained by PLD. This feature is an interesting characteristic of the PED process as the growth rate is known to be an experimental parameter limiting a broader use of the PLD technique for industrial trends.

According to atomic force microscopy experiments, the surface of ZnO films grown by PED is smooth with a mean roughness of 4.9 nm (RMS roughness of 7.9 nm) for a total thickness of 200 nm. The boundaries of the crystallites are also visible and their diameter can be estimated to 40 nm.

3.2. Film structure

The crystallization of the ZnO thin films on *c*-cut sapphire substrate was studied for the fixed experimental growth conditions leading to the growth of dense, smooth and stoichiometric films. The XRD diagram in the Bragg–Brentano geometry of ZnO thin films grown by PED on a *c*-cut sapphire substrate at 700 °C is shown in Fig. 2. A strong well-defined peak at $2\theta = 34.375°$ as well as a weak peak around 72° are observed on this diagram. It corresponds respectively to the (0002) and the (0004) diffraction peaks of the ZnO hexagonal wurtzite structure, indicating that the ZnO thin films are grown with the *c* axis normal to the sapphire substrate plane. This *c*-axis orientation of crystallites is classically observed for ZnO films whatever the growth method. Indeed, textured films are generally obtained when the plane parallel to the substrate has the lowest surface energy density [14]. In the case of ZnO which is a polar crystal (alternative stacking of Zn planes and O planes), the surface free energy of the (000l) plane has not a finite value. To limit the surface of such plane, the growth rate along the *c*-axis is increased and thus a columnar growth of ZnO crystallites is evidenced. The value of the *c* axis lattice parameter deduced from the diffraction pattern is $c = 0.52125$ nm. This value nearly reaches the bulk ZnO value $c_{bulk} = 0.52066$ nm. The estimated size of the ZnO crystallites through the Debye–Scherrer formula is 44 nm. The crystallite size in ZnO films grown by PLD is typically about 50 nm with the same columnar growth on sapphire [15].

The mosaic spread of this (0002) texture was studied by rocking curve measurements. The inset in Fig. 2 represents the (0002) rocking curve of the ZnO films on *c*-cut sapphire substrate. The FWHM of the rocking curve is only of 0.65° evidencing therefore a low mosaic spread of the crystallites according to the main axis growth and a high crystalline quality of the film similar to that of obtained in PLD films.

The (0002) texture observed in ZnO films suggests a possible epitaxial growth of the films. Pole figure measurements were performed to investigate the epitaxial relationships between the ZnO film and the sapphire substrate. Fig. 3 reports pole figures recorded for the $\{10\bar{1}3\}$ ZnO family planes ($2\theta = 62.86°$). Six well defined poles at a declination angle $\Psi = 32.5°$ are visible, indicating the existence of an epitaxial relationship between the film and the substrate. Moreover, three poles at a declination angle $\Psi = 22.5°$ are also observed, corresponding to the poles of the $\{01\bar{1}8\}$ planes of the *c*-cut sapphire substrate ($2\theta = 61.3°$).

Considering the sapphire substrate symmetry, only three poles should be observed for the $\{10\bar{1}3\}$ family planes of ZnO. This has already been observed and explained by the fact that the sapphire surface exhibit steps which induce an unconventional number of poles (6 poles 60° apart) and a symmetry of order 6 instead of 3 [16].

The comparison of the position of the six poles of the $\{10\bar{1}3\}$ ZnO planes, with the poles of the $\{01\bar{1}8\}$ family planes of the sapphire substrate, evidences a rotation of 30º of the ZnO axis with respect to those of the *c*-cut sapphire substrate. The following orientation relationship can therefore be inferred:

$$ZnO(0001)[2\bar{1}\,\bar{1}0] \,//\, Al_2O_3(0001)[1\bar{1}00]$$

Such an epitaxial growth is classically observed for the growth of ZnO thin films on *c*-cut sapphire substrates [17]. The 30° rotation between the 2 cells ensures the continuity of the hexagonal oxygen sublattice in the sapphire substrate and in the ZnO film. These orientations can be described in terms of "domain matching epitaxy" [18], which has been already used to describe the same epitaxial relationships evidenced in PLD ZnO films grown on sapphire at 700 °C [15].

In summary, regarding the main axis growth of the ZnO crystallites, their in-plane orientations with the sapphire substrate, and their estimated size in the several tens of nm range, the PED technique leads to ZnO films having a crystalline quality very similar to those obtained by PLD at the same substrate temperature.

3.3. Electrical measurements

The transport properties of the ZnO thin films grown by PED on *c*-cut sapphire substrates were investigated by resistivity and Hall effect measurements. The normalized resistivity as a function of the temperature is reported in Fig. 4. The resistivity decreases while the temperature increases revealing the semiconducting behavior of the thin film in the whole temperature range as it is classically observed with PLD ZnO films.

Hall effect measurements were performed at room temperature. It is found that the ZnO film is *n*-type and has a high amount of charge carriers ($n_e = 3.4 \times 10^{19}$ cm^{-3}). This is a very high value compared to undoped ZnO thin films prepared by PLD which are usually in the 10^{16} cm^{-3} range [7]. However, the electron mobility is only of 11.53 cm²/Vs at room temperature. This value of μ_e is far from the

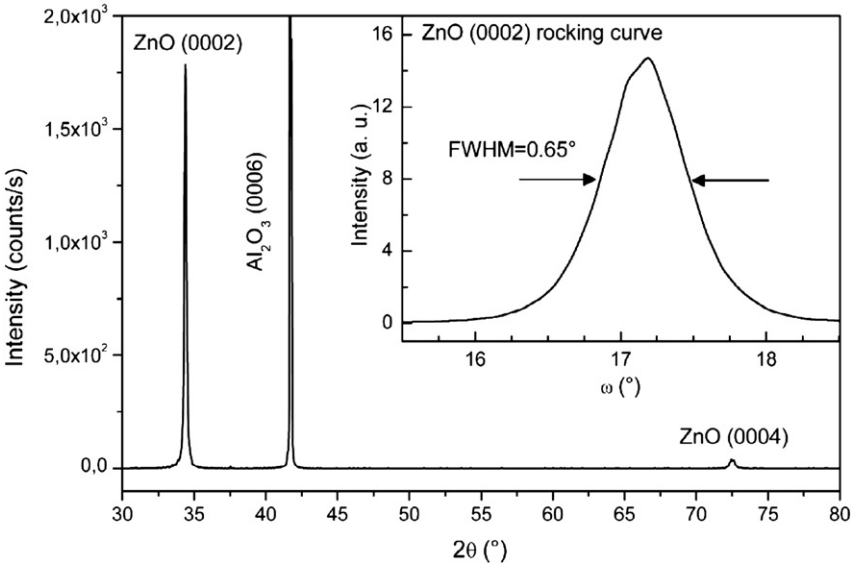

Fig. 2. θ–2θ XRD diagram of a ZnO thin film grown at 700 °C under 1.4×10^{-2} mbar argon pressure on *c*-cut sapphire substrate. The inset shows the corresponding rocking curves of the (0002) reflection.

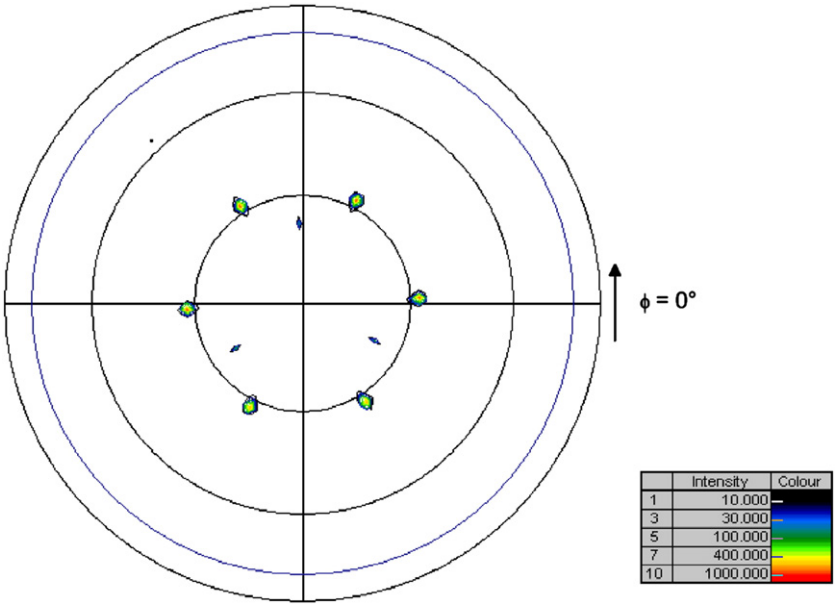

Fig. 3. Al_2O_3 $(01\bar{1}8)$ and ZnO $(10\bar{1}3)$ pole figure of a zinc oxide film grown by PED at 700 °C on a *c*-cut sapphire substrate.

expected theoretical value of 300 cm²/Vs for the bulk single crystal [19]. Thanks to the high density of charge carriers, the resistivity at room temperature is as low as 1.6×10^{-2} Ω cm. The good crystalline quality of the PED films and their stoichiometry (low concentration of oxygen vacancies) are in good agreement with a resistivity around 10^{-2} Ω cm. This value is similar to that of measured on ZnO films grown by PLD. Nevertheless, the higher mobility (above 100 cm²/Vs) leading to a resistivity of 10^{-2} Ω cm for PLD films can only be obtained for optimized PLD process such as a multi step growth, or buffer layers or even with substrates like $ScAlMgO_4$ to reduce the mismatch and increase the crystallite size [20].

The plot of $\ln(\rho)$ versus the reciprocal temperature for a ZnO thin film grown at 700 °C is presented in Fig. 5 and indicates an Arrhenius law versus temperature in the 230–300 K range. The activation energy (E_a) is determined from the slope of the linear region of the plot (inset in Fig. 5) and is 11.7 meV. From this activation energy, a donor level located at $E_D = 2E_a = 0.024$ eV below the bottom of the conduction band can be deduced.

A clear deviation from the Arrhenius law is observed when the temperature is below 230 K. This suggests that transport properties could not be anymore correctly described by thermally activated conduction. Classically, it is generally assumed that the transport properties of such films can be described at low temperature range by the variable range hopping model (VRH), in which electrons hop between deep donor states [21]. In this model, the resistivity follows the expression:

$$\rho = \rho_0 \times \exp\left[\left(\frac{T_0}{T}\right)^{1/4}\right] \quad (1)$$

where ρ_0 is a function of $T^{1/2}$ and T_0 is constant. According to Eq. (1), it follows that $\ln(\rho T^{-1/2})$ is proportional to $T^{-1/4}$. This relation is presented in Fig. 6. The data can be correctly adjusted by a linear variation in the low temperatures domain which confirms the VRH model at low temperature (below the Arrhenius activated regime) in the films, in the short range of 150–120 K. These transport properties

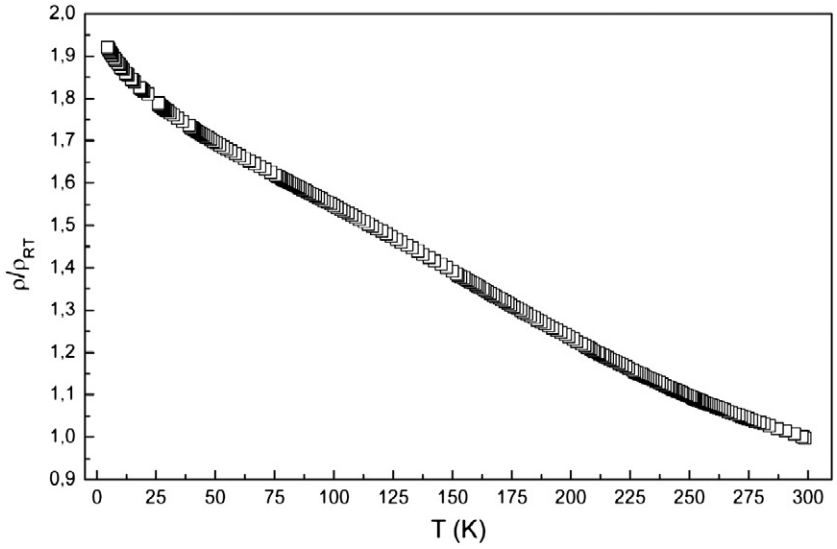

Fig. 4. Temperature dependence of the normalized electrical resistivity ($\rho(T)/\rho_{300\ K}$) for the ZnO thin films grown on *c*-cut sapphire substrates at 700 °C.

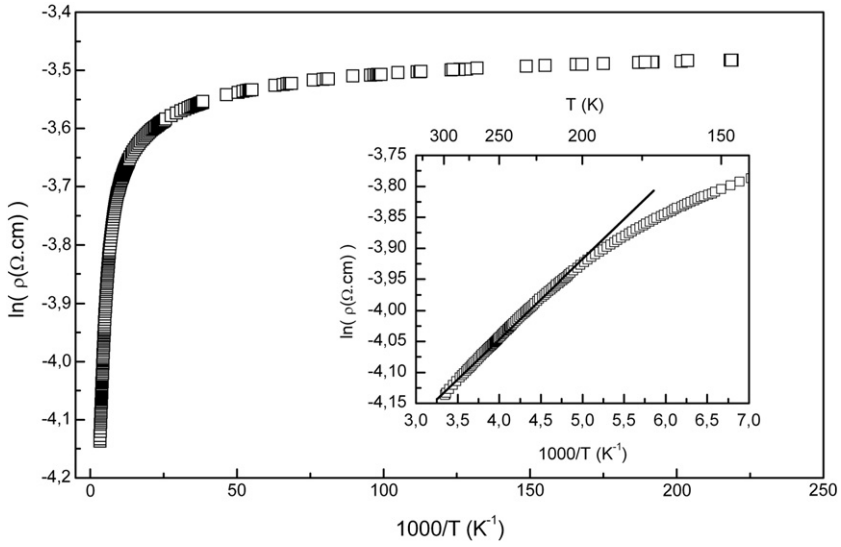

Fig. 5. Arrhenius plot of the resistivity of a ZnO thin film grown at 700 °C as a function of the reciprocal temperature. The inset shows the linear region (230–300 K) used for the determination of the activation energy.

of ZnO thin films are not PED specific since the transition between the classical thermally activated conduction to the variable range hopping mechanism has already been reported for ZnO films prepared by other methods and not fully explained. However, the temperature range in which the VRH model holds is quite reduced, and the temperature domain ranging from 150 to 230 K cannot be explained by the VRH model or the Arrhenius law. Such temperature dependent resistivity curve can be originated from the high density of charge carriers observed in these films linked to the oxygen vacancies and/or impurities which induces localized states. A metallic behavior of undoped ZnO PED film displaying a density of carriers in the $1-3\times10^{20}$ cm^{-3} has been recently observed [22].

3.4. Optical properties

Optical properties of ZnO thin films grown by PED on *c*-cut sapphire substrate at 700 °C were studied by absorption measurements in the 190–900 nm wavelength range. Films are well transparent since the transmittance reaches 90% in the visible range for wavelength above 400 nm. A strong decrease of the transmittance is also observed around 370 nm which is consistent with good quality ZnO thin films [23]. This cut-off of the transmittance corresponds to band to band absorption. The energy gap was obtained by applying the Tauc model to absorption measurements [24]. In this model, the variation of the absorption coefficient α in the strong absorption range ($\alpha<10^4$ cm^{-1}) is linked to the energy gap E_g of the material by the following expression:

$$\alpha = B \times \frac{E-E_g}{E}^{m} \quad (2)$$

In the above equation E is the photon energy, B is a constant and the allowed values for m are 1/2 for an allowed direct transition, 3/2 for a forbidden direct transition and 2 and 3 for an allowed and a forbidden indirect transition respectively. Since ZnO is a direct band gap semiconductor ($m=1/2$), Fig. 7a shows $(\alpha E)^2$ as a function of the photon energy E. The extrapolation of the linear region of the curve up to $\alpha=0$ gives the value of E_g. From Fig. 7a, the optical band gap of ZnO thin films grown by PED is 3.28 eV. This value is in the same range

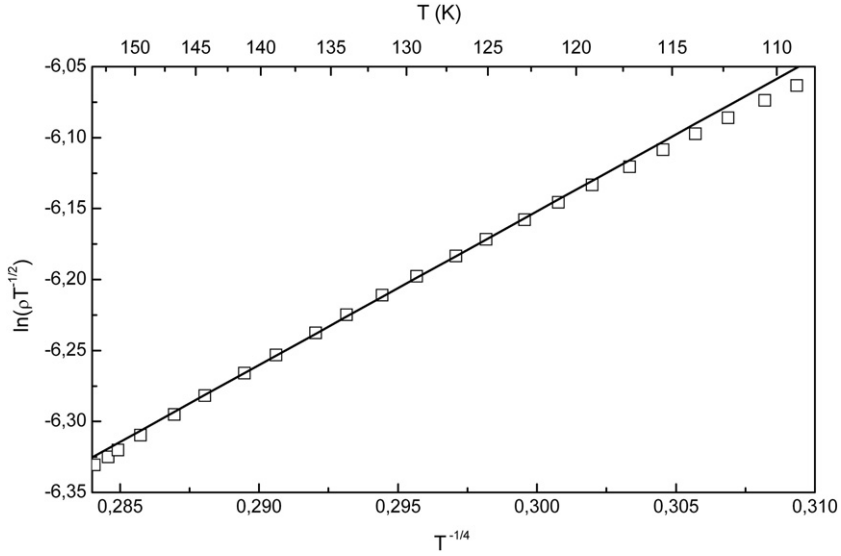

Fig. 6. Variation of $\ln(\rho T^{-1/2})$ versus $T^{-1/4}$ for a ZnO film grown at 700 °C. The linear fit (solid line) indicates the temperature range where the VRH conduction applies.

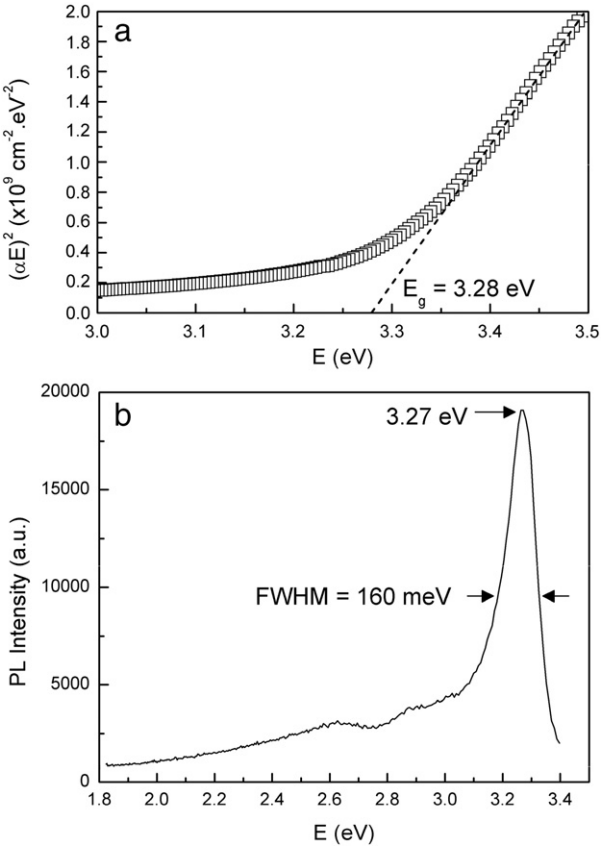

Fig. 7. a) Tauc plot of the absorption coefficient of ZnO film grown on *c*-cut sapphire at 700 °C under 10^{-2} mbar Ar. The dash line represents the extrapolation to zero of the linear part of the curve corresponding to the optical band gap of the film. b) Room temperature photoluminescence spectrum of a ZnO film grown on *c*-cut sapphire by PED at 700 °C.

than that of observed in ZnO films grown by PLD [25] or by other deposition techniques (sputtering, solgel [26]).

Fig. 7b shows the normalized photoluminescence spectrum recorded at room temperature. An intense near band edge emission is observed at 3.27 eV with a weak blue-green band (or deep level emission) at about 2.6 eV. The lower intensity of the latter indicates a high quality of the ZnO films grown by PED in Ar at 700 °C even without post-deposition thermal treatment under oxygen. The intensity ratio of the near band edge emission to deep-level emissions is about 7 at room temperature. The deep-level emission is usually related to structural defects but in the case of ZnO films grown on *c*-cut substrate the lattice mismatch plays an important role even for epitaxial thin films grown by PLD [27]. The long tail extending from the near band edge emission, which is usually caused by band structure deformation resulting from lattice deformation [17], is confirmed by the investigation of structural properties (cf. Section 3.2).

In relation to ZnO films grown on *c*-plane sapphire substrates by PLD [28] the as-deposited PED ZnO films show good optical properties. To improve them, a high temperature annealing treatment in oxygen is probably needed as it is classically performed on ZnO films grown by various techniques. Nevertheless it was not the aim of this work since the physical properties of the ZnO PED films are compared with those of as-deposited ZnO PLD films. These results therefore indicate that PED is a viable technique for producing high quality epitaxial thin films of ZnO for optical applications.

Finally, it has to be noticed that this band gap value is slightly lower than the one of bulk ZnO (3.3 eV). According to the Burstein–Moss effect, the high density of charge carriers is supposed to create donor states in the conduction band which limits thermal or optical excitation. As a consequence the band gap value would be supposed to increase (blue shift). As this effect is not observed for our films, the optical absorption edge may be modified by the change of interactions between donors and host crystal. This phenomenon induces a band gap shrinkage evidenced by a shift of the measured optical gap toward the lowest energy. The competitive effects of the Burnstein–Moss shift and the band gap shrinkage has already been observed in heavily defect-doped ZnO films [29].

4. Conclusions

In this work, we have demonstrated the possibility of growing dense, smooth, stoichiometric and crystalline zinc oxide films by the pulsed electron beam deposition method using a channel-spark discharge as the pulsed electron source. These ZnO films obtained by PED were found to grow epitaxially on *c*-cut sapphire substrates at 700 °C, with the classical epitaxial relationship also observed for ZnO films grown by the well-known PLD method under similar conditions. In the same way, the optical and electrical properties of PED and PLD ZnO films are very similar.

These results demonstrate the ability of PED to grow high crystalline quality oxide films showing the same functional properties than films grown by other methods. In addition, the PED technique highlights interesting advantages regarding the experimental process in term of growth rate (10 times higher than that of PLD) and the transfer of the target composition which does not require in the setup the incorporation of oxygen at a controlled pressure.

The PED ZnO films show a resistivity of $10^{-2}\,\Omega$cm at room temperature. Such value classically observed for undoped ZnO films is due to charge carriers with a relatively high density (3.4×10^{19} cm^{-3}) but with a low mobility (11.53 cm²/Vs). This could be due to the fact that these films are composed of closely packed hexagonal columns separated by grain boundaries, which are usually thought to be detrimental for high carrier mobility. The temperature dependent resistivity curves of the PED films highlight a semiconducting behavior but cannot be explained by a simple law : at high temperature (above 230 K) the resistivity follow the Arrhenius law while the VRH model may be applied at low temperature (below 150 K). The optical band gap of PED ZnO films is close to the bulk value. Nevertheless, more detailed investigations have to be made to explain the shift of the optical edge observed on PED ZnO films according to the density of charge carriers and its consequence on the Burstein Moss effect and/or the band gap shrinkage. PED ZnO films grown at different temperatures appear therefore as good candidates to go deeper on this subject.

Acknowledgements

The authors are grateful to S. Kilburger for the AFM experiments and to I. Enculescu for the photoluminescence measurements.

References

[1] G. Müller, M. Konijnenberg, G. Krafft, C. Schultheiss, in: F.C. Matacotta, G. Ottaviani (Eds.), Science and Technology of Thin Films, World Scientific Publ. Co. PET. LTD, 1995.
[2] M. Nistor, N.B. Mandache, J. Perrière, J. Phys. D Appl. Phys. 41 (2008) 165205.
[3] M. Nistor, N.B. Mandache, J. Optoelectron. Adv. Mater. 7 (2005) 1619.
[4] S. Tricot, N. Semmar, L. Lebbah, C. Boulmer-Leborgne, J. Phys. D Appl. Phys. 43 (2010) 065301.
[5] S. Tricot, C. Boulmer-Leborgne, M. Nistor, E. Millon, J. Perrière, J. Phys. D Appl. Phys. 41 (2008) 175205.
[6] V. Craciun, S. Amirhaghi, D. Craciun, J. Elders, J.G.E. Gardeniers, I.W. Boyd, Appl. Surf. Sci. 86 (1995) 99.
[7] U. Ozgur, Ya.I. Alivov, C. Liu, A. Teke, M.A. Reshchikov, S. Dogan, V. Avrutin, S.-J. Cho, H. Morkoc, J. Appl. Phys. 98 (2005) 041301.
[8] D.C. Look, Mater. Sci. Eng. B 80 (2001) 383.
[9] H. Hosono, Thin Solid Films 515 (2007) 6000.
[10] A. Ohtomo, M. Kawasaki, Y. Sakurai, Y. Yoshida, H. Koinuma, P. Yu, Z.K. Tang, G.K.L. Wong, Y. Segawa, Mater. Sci. Eng. B 54 (1998) 24.
[11] H.L. Porter, C. Mion, A.L. Cai, X. Zhang, J.F. Muth, Mater. Sci. Eng. B 119 (2005) 210.

[12] L.R. Doolittle, Nucl. Instrum. Methods Phys. Res. Sect. B 9 (1985) 344.
[13] D.S. Williams, F.A. Baiocchi, R.C. Beairsto, J.M. Brown, R.V. Knoell, S.P. Murarka, J. Vac. Sci. Technol. B 5 (6) (1987) 1723.
[14] N. Fujimura, T. Nishihara, S. Goto, J. Xu, T. Ito, J. Cryst. Growth 130 (1993) 269.
[15] J. Perrière, E. Millon, W. Seiler, C. Boulmer-Leborgne, V. Craciun, O. Albert, J.C. Loulergue, J. Etchepare, J. Appl. Phys. 91 (2002) 690.
[16] J. Guo, H.L.M. Chang, D.J. Lam, Appl. Phys. Lett. 61 (1992) 3116.
[17] Y. Chen, D.M. Bagnall, H.-J. Koh, K.-T. Park, K. Hiraga, Z. Zhu, T. Yao, J. Appl. Phys. 84 (1998) 3912.
[18] J. Narayan, B.C. Larson, J. Appl. Phys. 93 (2003) 278.
[19] J.D. Albrecht, P.P. Ruden, S. Limpijumnong, W.R.L. Lambrecht, K.F. Brennan, J. Appl. Phys. 86 (1999) 6864.
[20] A. Ohtomo, K. Tamura, K. Saikusa, K. Takahashi, T. Makino, Y. Segawa, H. Koinuma, M. Kawasaki, Appl. Phys. Lett. 75 (1999) 2635.
[21] N.F. Mott, J. Non-Cryst. Solids 1 (1968) 1.
[22] M. Nistor, F. Gherendi, N.B. Mandache, C. Hebert, J. Perriere, W. Seiler, J. Appl. Phys. 106 (2009) 103710.
[23] E. Millon, O. Albert, J.C. Loulergue, J. Etchepare, D. Hulin, W. Seiler, J. Perrière, J. Appl. Phys. 88 (2000) 6937.
[24] J. Tauc, in: F. Abelès (Ed.), Optical properties of solids, 1972.
[25] J.N. Zeng, J.K. Low, Z.M. Ren, T. Liew, Y.F. Lu, Appl. Surf. Sci. 197–198 (2002) 362.
[26] Y. Natsume, H. Sakata, Mater. Chem. Phys. 78 (2002) 170.
[27] E.S. Shim, H.S. Kang, J.S. Kang, J.H. Kim, S.Y. Lee, Appl. Surf. Sci. 186 (2002) 474.
[28] J.F. Muth, R.M. Kolbas, A.K. Sharma, S. Oktyabrsky, J. Narayan, J. Appl. Phys. 85 (1999) 7884.
[29] A.P. Roth, J.B.N. Webb, D.F. Williams, Phys. Rev. B 25 (1982) 7836.